CONFERENCE PRE-PRINT

DIVERTOR FLUX CONTROL BY RMP ELM SUPPRESSION AND RADIATIVE DIVERTOR OPERATION IN EAST H-MODE WITH TUNGSTEN PLASMA FACING COMPONENTS IN SUPPORT OF ITER NEW RESEARCH PLAN

M. JIA

Institute of Plasma Physics, Chinese Academy of Sciences Hefei, China Email: jiamanni@ipp.ac.cn

Email: Jumami Cippiaci

H. YANG

Institute of Plasma Physics, Chinese Academy of Sciences Hefei, China

A. LOARTE

ITER Organization

S. GU, Y. SUN, X. GONG, J. QIAN, L. ZHANG, K.D. LI, T. ZHANG, L. WANG, L. MENG, Q. MA, X. WU, P. XIE, G. ZUO, H.H. WANG AND EAST TEAM Institute of Plasma Physics, Chinese Academy of Sciences Hefei, China

Y. LIANG Forschungszentrum Jülich Jülich, Germany

Y.Q. Liu General Atomics San Diego, CA, USA

Aabstract

Effective divertor flux control has been achieved in EAST H-mode plasmas under high-Z metal (tungsten/ molybdenum) wall conditions, employing plasma-facing components (PFCs) that include tungsten (W) upper and lower divertors, tungsten main limiters, and a molybdenum (Mo) first wall with low boron coverage. To mitigate transient heat loads caused by Type-I Edge Localized Modes (ELMs), n = 2 Resonant Magnetic Perturbations (RMPs) were applied, achieving full ELM suppression. The impact of n = 2 RMP ELM suppression on H-mode energy and particle confinement was limited to less than 10%, while core tungsten concentrations remain effectively controlled. For steady-state divertor heat load reduction, nitrogen (N₂) injection into the divertor during n = 2 RMP operation enabled radiative divertor performance, successfully divertor detachment at both the original and splitting strike points. These results confirm the compatibility of ELM-controlled H-mode operation with radiative divertor scenarios in a high-Z metal wall environment and provide a validation for ITER new research plan which has been decided to transfer the first wall material from beryllium to tungsten.

1. INTRODUCTION

Externally applied 3D resonant magnetic perturbation (RMP) have been widely found to be beneficial for the control of edge localized instabilities in tokamak, and will be implemented in ITER. Meanwhile, the implications of RMP application are introducing new influence on the tokamak plasma, such as the change of the magnetic topology itself, its impact on the stead state edge plasma and the particular focus on the divertor target power loads. A substantial part of power exhaust can be deposited transiently during the impact of Edge Localized Modes (ELMs), typically, in the order of 10 MJm^{-2} for ITER high confinement mode (H-mode) operation[1, 2]. Application of RMP field is a proven method for suppressing Type-I ELMs in H-mode plasma [3], which could be used to eliminate these unexpected transient heat flux bursts. Furthermore, even in the absence of such large transient event, there has to be a reliable mechanism for the plasma escaping confinement to exhaust its

energy before reaching the divertor targets [1]. Application of RMP fields can break the tokamak plasma symmetry, cause the edge stochasticity and alter the separatrix. Particularly, the pattern of divertor power loads is essentially determined by the separatrix, which splits into two distinct branches as a results of small RMP to an axisymmetric equilibrium field. Thus, RMP fields could redistribute the deposition patterns of stationary particle and heat fluxes onto the divertor plate [4, 5]. This brings potential questions about achieving full detachment under 3D magnetic configuration. Modeling for ITER suggests that the increase of gas puffing creates a localized detachment in near-separatrix locations while no detachment in off-separatrix lobes after after RMP field breaking the axisymmetric heat flux distribution within the scrape-off layer (SOL) [6]. Achieving a detached divertor plasma is crucial for reactor-relevant tokamak devices to handle power exhaust and protect plasma-facing components (PFCs) [1]. In a detached regime, the electron temperature at the divertor target can drop to ~ 5eV or below, and the divertor peak heat flux is reduced by more than 50% through enhanced volumetric radiation [7]. This is especially important for ITER with W first walls (sputtering threshold ~8 eV). Nitrogen gas seeding has been demonstrated an effective method to increase divertor radiation to achieve detachment. In some cases, nitrogen gas seeding could form a cold, dense, and highly radiative plasma region above the X-point of the single-null magnetic configuration in a tokamak plasma, called X-point radiator (XPR). Such properties allow it to buffer the heat exhaust and protect the PFC. Therefore, the XPR regime is inherently detached and can even be controlled to reach an ELM-suppressed regime [8].

It has been found that RMP led to keep core tungsten levels "effectively controlled" [9]. No strong tungsten peaking was observed, consistent with RMP-induced reduction of the total tungsten source from plasma wall interactions (PWI). On the other hand, light impurity gas seeding, such as nitrogen or methane, has been considered as an effective radiator for edge plasma that protects against the overheating of divertor target [10]. In this paper, we reports the first experimental observation of a X-point radiative detachment divertor plasma under sustained RMP application in EAST. The observations of XPR state and normal radiative divertor plasmas are displayed during applying RMP fields together with N_2 puffing. When the plasma is driven into a XPR state: the entire divertor target is below the tungsten sputtering temperature and the heat fluxes decreased significantly at both near- and off-separatrix lobes. Though, in the moderate nitrogen gas rate, the XPR does not achieve, the normalized energy confinement H_{98} is not compromised. Core tungsten accumulation of these two shots are both weakened. These results demonstrate that the RMP-induced ELM control regime can be compatible with detachment in a metallic-wall tokamak.

2. DETACHMENT WITH INCREASING OF NITROGEN RADIATION DURING N=2 RMP

2.1. ELM suppression by n=2 RMP with metal wall

One example of the n=2 RMP ELM suppression discharge (#132837) is shown in Fig.1, which compares with a type-I ELMy H-mode shot (#132679) without RMP application. The background plasma scenario in these experiments was a near double-null with dominant lower X-point and with $I_p \sim 450$ kA and $B_t \sim 2.45$ T ($q_{95} \sim 6$). For achieving type-I ELMy H-mode, the central Electron Cyclotron (EC) heating is set to be 1.5MW, and other heating power were provided by Neutral Beam Injection (NBI) of 1.37MW. As the type-I ELMy confinement is highly sensitive with the gap between plasma and the W limiter, the outer mid-plane distance between the separatrix and the limiter is fixed at about 7.5cm. In shot 132837, n = 2 RMP was applied from 4.2 to 5.6s with the upper-lower phase difference of about -150 degree. After RMP application, the ELM mitigation state was reached and the energy confinement (indicated by H_{98} factor here) was reduced stepwise from 0.9 to 0.72. At about 4.9s, there is a non-linear transition from ELM mitigation to suppression state and the H_{98} increased to 0.87, only 3% less than that before RMP application. The particle confinement is not affected by the ELM control. The main impact is on the central ion temperature which decreases when ELM suppression is achieved. During RMP application, there is no obvious accumulation of W in the core and the W level at the divertor plate is reduced. Previous results in EAST show that RMP effects on W reduction are closely related with rotation braking and the impact of RMP induced neoclassical toroidal viscosity (NTV) on low charge states of W is greater than that on high charge states.

2.2. Detached plasma by nitrogen puffing during RMPs

To explore the compatibility of H-mode confinement, ELM control and the radiative divertor operation, N_2 was injected from the divertor region as impurity during n=2 RMP application. The background plasma is updated with $I_p \sim 500$ kA and $B_t \sim 2.45$ T in latest 2025 experiments campaign. The plasma was heated by 1.35 MW EC and 1.4 MW NBI with line averaged density < ne > of about $4.8 \times 10^{19} m^{-3}$. Different from previous type-I ELM suppression discharges, the background plasmas are a type-II ELMs with RMP application. The evolution of plasma parameters of discussed discharges are shown in Fig.2, respectively. Compared to moderate N_2 seeding rate shot #154627, shot #154624 shows clear decrease of plasma density and stored energy after the larger N_2 seeding, and more effective ion number, as shown in Fig.2 (a), (c) and (f), respectively. Obviously, though larger N_2 rate shot #154624 brings more reduction of confinement, it can accomplish more significant decrease of LO-divertor target temperature compared to shot #154627, seen in Fig.3. Fig.3 is the origin pictures, captured by HIR, which are displaying different divertor heat fluxes conditions. Each row of Fig.3 from left to right is symmetric condition (origin strike point), switching on RMP (splitting strike point), beginning of N_2 seeding (weaken the heat fluxes) and after

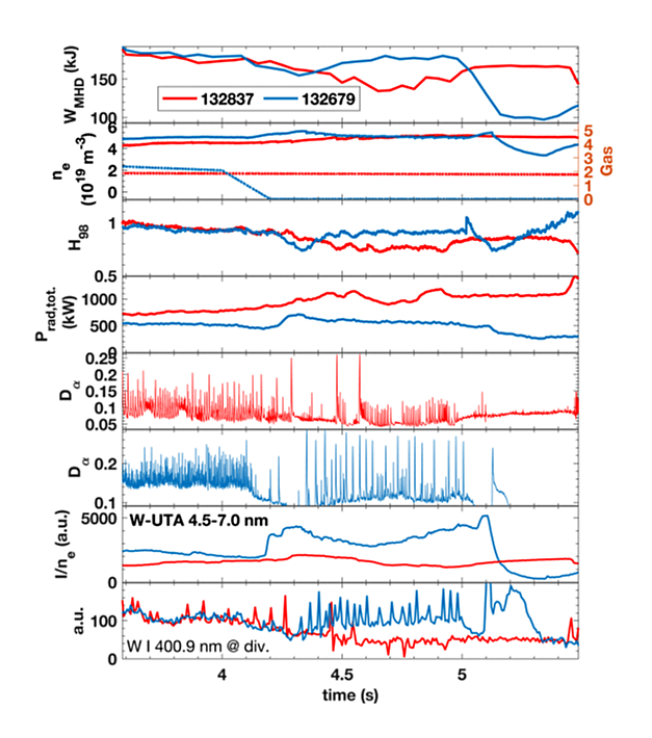


FIG. 1. Impact of ELM mitigation and ELM suppression with n = 2 RMPs on H-mode performance with high-Z metal wall in EAST.

the N₂ seeding (achieving detachment or partial detachment). Based on the above results mentioned, shot #154624 exhibits a more pronounced mitigation effect on heat fluxes compared to shot #154627; however, it also imposes a more substantial impact on plasma confinement. N_2 is seeding after the first RMP rotating cycle at a puffing rate of approximately 6.1×10^{20} particles/s for shot #154624 and 4.1×10^{20} particles/s for #154627 during 6.0–7.5 s, as shown in Fig. 2(g). As shown in Fig. 4, detached plasma in the LO-div was successfully established with the N₂ seeding. With the N_{II} radiation intensity increasing and saturating at $t_a \sim 6.7s$, the near- and off-separatrix heat fluxes measured by the FIR camera are reduced by more than 90% nearly vanished, as shown in Figs.4(c)-(d). Meanwhile, Fig.4(b) shows the roll-over of particle fluxes at vertical target. The nitrogen radiation zone is initially localized in the divertor volume near the X-point (N_{II}) . The dominant nitrogen radiation moves upward with continued N_2 puffing. And then, strong N_{VI} radiation appeared in the mid-plane location, provided by EUV, as shown in Fig.3(e), signifying enhanced nitrogen ionization within the confined plasma. At $t_b \sim 7.3s$, the confined plasma transforms into X-point radiator region, which could be supported by the change of the main radiation location as shown in the Fig.5, bringing full detachment in the divertor target [10]. It shows a strong radiation in the confined region close to the X-point, which may be mainly from N_{VI} ionization state, which is usually fully ionized in the pedestal region. As shown in Fig.5, there is a significant increase of radiation near the X-point region after 7.3 s and a decrease in the core corresponding to the rise of N_{VI} in the edge and the reduction of W-UTA in the core plasma, respectively, as shown in Fig.7(b)-(c). The retention of nitrogen radiation contributed to maintaining the detached state. Even after the cessation of N₂ injection at 7.5 s, detachment was sustained until approximately $t_c \sim 8.2$ s. The D_{γ}/D_{α} ratio is also increasing, indicating the onset of volume recombination, which usually coincides with the detachment [11]. The higher recombination rate is usually occurred with the lower level electron temperature in the divertor volume. Though, due to the damage of divertor probes, the $T_{e,div}$ on the horizontal target can not acquire, the $T_{e,div}$ on the vertical target are still below to ~ 5 eV when the onset of detachment, as shown in Fig.3(f). It also is below the sputtering electron temperature of tungsten, significantly reducing the tungsten source from divertor targets, as proven in Fig.7(d). Based on these results, N2 seeding during the application of RMPs can effectively decrease the power load to the divertor and the main tungsten source from divertor target, what is, provide a enough protect to the safety operation. Shot #154624 demonstrates that N₂ seeding during the application could simultaneously mitigate the near- and off-separatrix heat loads, achieving XPR and detachment, however, it brings an about 15% degradation of store energy, as shown in Fig.2(c). Thus, a lower N_2 puffing rate $(4.1 \times 10^{20} p./s)$ comparing to shot #154624 is used for shot #154627, which shows similar phenomena but fewer impact on the stored energy, as shown in Fig.6. Effectively cooled plasma in the LO-div is also successfully established during the N₂ seeding phase. The heat fluxes measured by the FIR camera are reduced by more than 75%, and the characteristic near- and off-separatrix lobes vanished as N_{II} radiation intensity increased, as shown in Figs.6(c)-(d). Fig.6(b) shows the time evolution of particle fluxes, which is increasing with N₂ seeding. With the onset of N₂ seeding, N_{II} radiation intensity rapidly increases and then saturates; concurrently, a significant drop in heat fluxes at $t_1 \sim 7.1$ s. The ratio of D_{γ}/D_{α} is also flatten from this moment, seen in Fig.6(d) blue line. The electron temperature measured

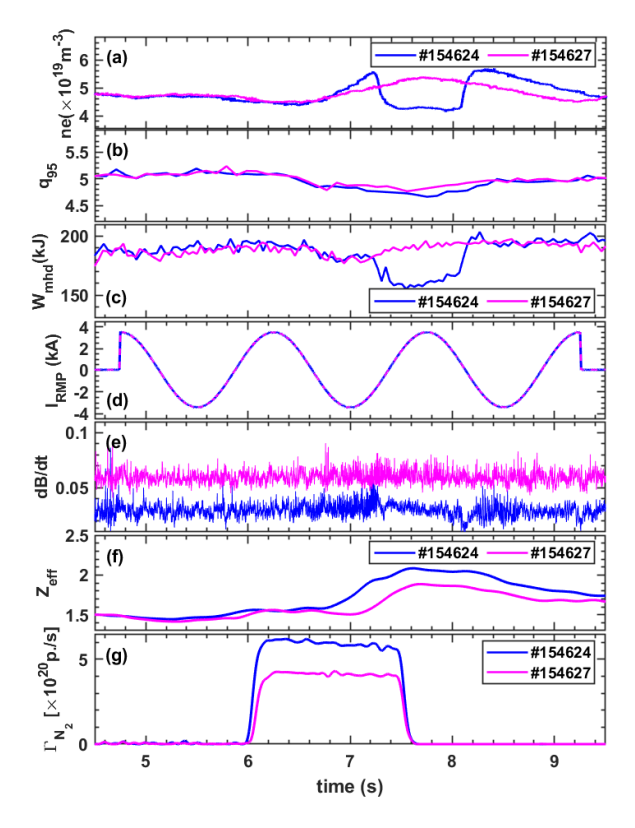


FIG. 2. The 0.75 Hz rotating RMP for #154624𥰃 during 4.75-9.25 s. Temporal evolution of (a) the plasma line density; (b) the safety factor q_{95} (c) stored energy; (d) RMP coil current and (e) the ELM performances represented by dB/dt; (f) the effective ion number Z_{eff} and (g) N_2 gas puffing rate. The blue line represents #154624 and magenta #154627.

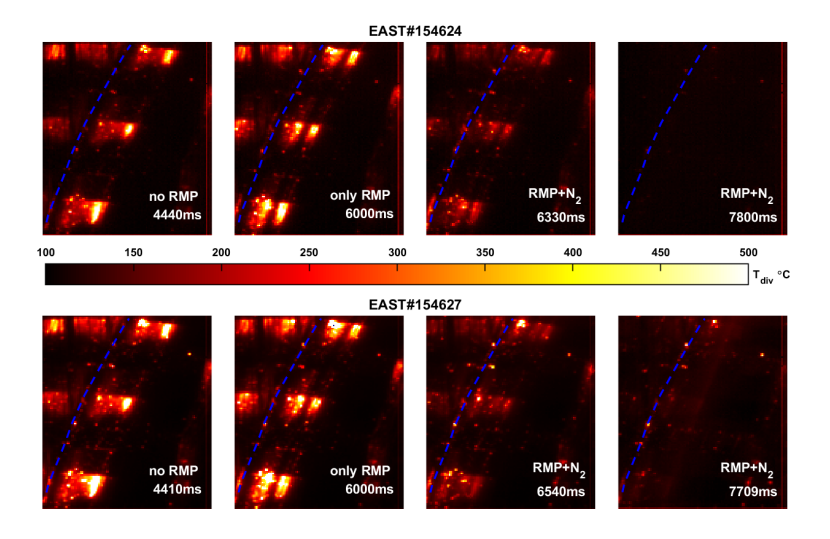


FIG. 3. The original pictures of two discharges captured by FIR camera for different plasma states. First row for shot #154624 and second row for shot #154627, blue dashed line represents the corner which divides divertor into horizontal and vertical targets.

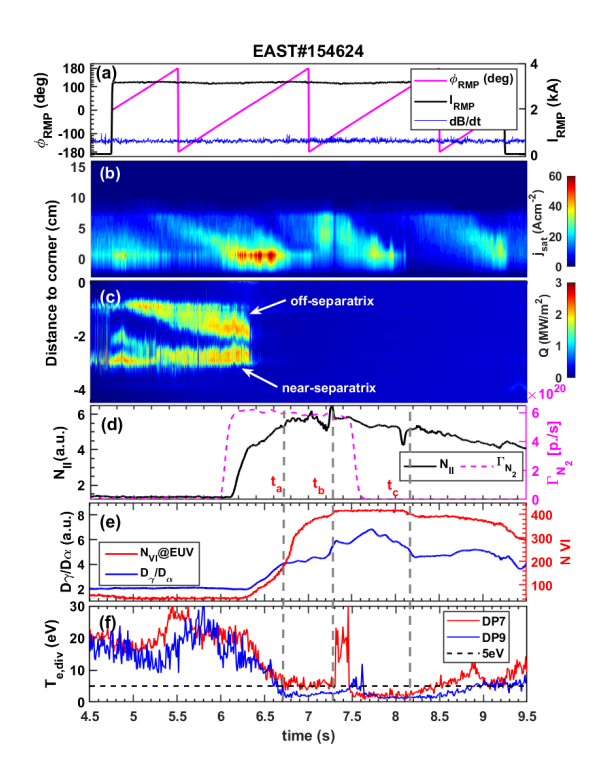


FIG. 4. Discharge #154624 temporal evolution of (a) the RMP coil current phase (black) and ELM performance (blue); (b) the saturated ion fluxes measured by divertor probes on LOdiv vertical plate and (c) heat fluxes distribution by FIR camera on LOdiv horizontal plate; (d) N_2 puffing rate (magenta dashed line) and intensity of N_{II} (black); (e) D_{γ}/D_{α} (black) and intensity of N_{VI} (red) in the bulk plasma monitored by EUV and (f) $T_{e,div}$ on the vertical plate, the abnormal data around 7.3-7.5 s may be caused by the electric arc at the probes.

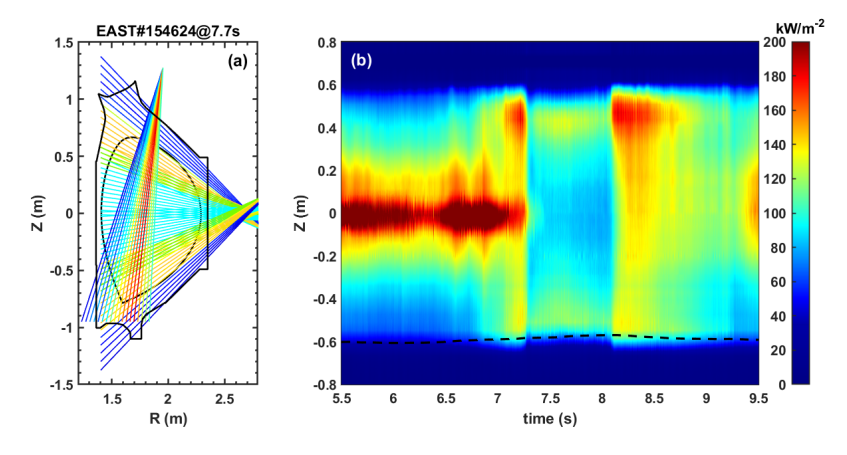


FIG. 5. (a) AXUV line of sight intensity with a strong XPR at 7.7 s in shot #154624. (b) The time evolution of chord-integrated radiation power intensity measured by AXUV horizontal chords. The vertical coordinate in (b) corresponds to the height (value of Z) on EAST at R = 1.85 m. The black dashed line in (b) corresponds to the position of the lower X-point.

from the LO-div vertical target (DP7&9) decreases from \sim 30 eV to below 5 eV, as shown in Fig.6(f). These observations might support the partial detachment in shot #154627 plasma persisting until $t_2 \sim$ 8.1 s. However, the lack of $T_{e,div}$ on the divertor horizontal target, near the OSP, makes no strong evidence to support detached plasma in this case. In EAST, the dominant

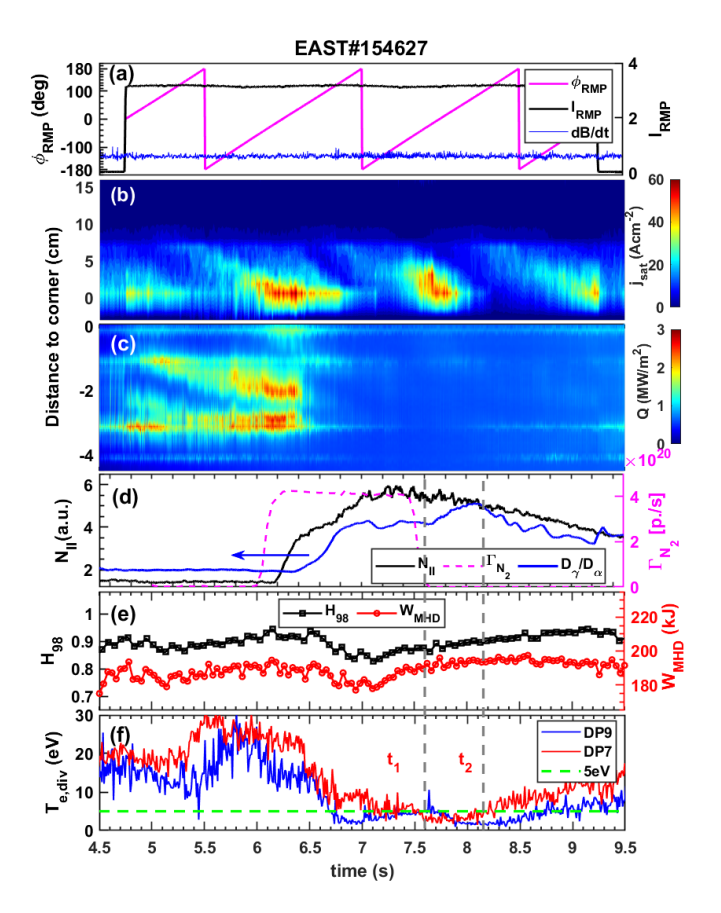


FIG. 6. (a) AXUV line of sight intensity with a strong XPR at 7.7 s in shot #154624. (b) The time evolution of chord-integrated radiation power intensity measured by AXUV horizontal chords. The vertical coordinate in (b) corresponds to the height (value of Z) on EAST at R = 1.85 m. The black dashed line in (b) corresponds to the position of the lower X-point.

source of W impurity originates from the divertor targets. Previous studies have shown that the application of RMP can help reduce W accumulation in the core plasma [9]. The present study indicates that divertor detachment, achieved during RMP application combined with N₂ puffing, is compatible with decreasing W influx and accumulation. As shown in Fig. 7(c)&(d), this reduction is attributed to rapid cooling of the divertor plasma due to nitrogen radiation, which reduces sputtering of tungsten from the divertor plates. The intensity of tungsten radiation at the divertor volume decreased markedly after the N_2 gas puffing by $\sim 6.4s$, indicating that there does not induce extra tungsten erosion. Concurrently, the tungsten concentration in the core plasma monitored via W - UTA line radiation also decreases after the application of RMPs and drops further upon when achieving complete detachment at $t_a \sim 7.1s$ (Fig.7(c)) for #154624 and cooled plasma state at $t_1 \sim 7.6s$ for #154627, aligning with the radiation profiles recorded by the AXUV (Fig.6(b)). With the application of RMP and N_2 puffing, the dominant radiation shifts to the plasma edge region Fig.6(b). The observed decrease in tungsten radiation is directly associated with the reduction in tungsten peaking in the core plasma (Fig.8). This might result from enhanced outward transport of tungsten ions, facilitated by increased nitrogen content in the confined region [12], rather than the decrease of the source of tungsten from the divertor, which remains at a low level (Fig. 7(d)). The presence of light impurities like nitrogen could modify edge transport properties and reduce inward tungsten convection, thereby mitigating core tungsten accumulation partly. These results suggest that integrating RMP-induced ELM control with nitrogen-induced divertor detachment not only helps manage divertor heat fluxes but also contributes to controlling core tungsten content. These observations of synergy effect may provide some support relevance for ITER and future reactors operating with full-W plasma-facing components.

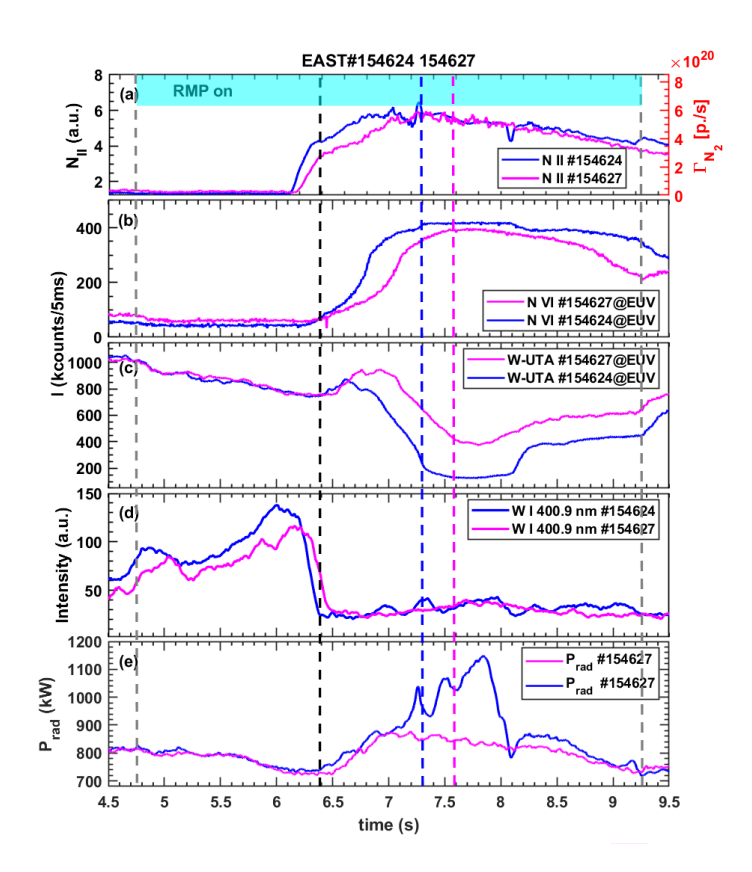


FIG. 7. Temporal evolution of shot #154624 (blue) and #154627 (magenta), respectively. (a) intensity of N_{II} emission line in the divertor region; (b) intensity of N_{VI} emission line in the bulk plasma and (c) core tungsten radiation W-UTA; (d) tungsten radiated intensity in front of divertor targets by div-W and (e) total radiated power (P_{rad}) .

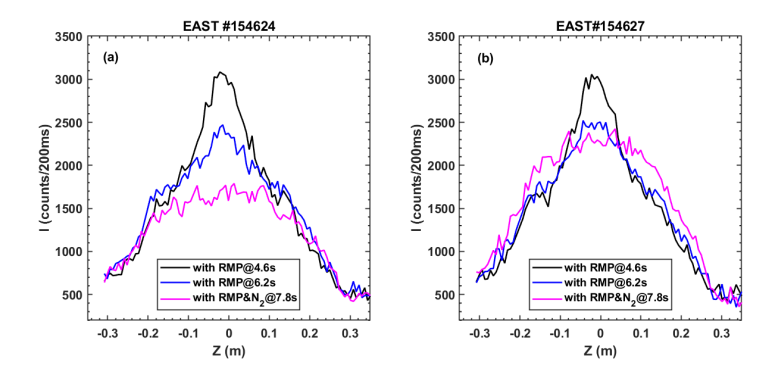


FIG. 8. The profiles of W^{45+} of shot #154624 (a) and shot #154627 (b). At the beginning of applying RMP @4.8 s (black), with RMP @6.2 s (blue) and with RMP+ N_2 @ 7.8 s (magenta).

3. SUMMARY

For the first time in EAST, it demonstrates that a detached divertor regime with low power load distributed over both the toroidal and poloidal divertor target surfaces can be achieved by N_2 puffing during the application of n = 2 rotating RMP. The full detachment occurs by XPR with large N2 puffing rate and cooled plasma state achieves by moderate puffing rate, which maintaining good global energy confinement. Both of these two condition could avoid tungsten peaking in the core plasma. In this campaign, N2 puffing combined with RMP fields successfully induced detachment at the lower outer divertor, marked by a reduction in local heat flux on the near- and off-separatrix lobes by more than 75% and a drop in $T_{e,div}$ below 5 eV in the vertical target (far to OSP). These results confirm that nitrogen-induced detachment extends not only to the OSP but also to off-separatrix lobes. Tungsten accumulation in the confined plasma is significantly reduced in this $RMP + N_2$ operation scenario. The application of RMP fields induces a prompt and continuous reduction of tungsten levels. On the other hand, N_2 seeding reduces the divertor electron temperature, suppressing divertor tungsten sputtering, a major source of W impurities. A clear anti-correlation between core tungsten and edge nitrogen radiation intensity supports the hypothesis that light impurity seeding improves tungsten control. Together, the application of RMP and N_2 puffing exhibit a synergistic effect in minimizing core tungsten peaking while enabling cooled plasma in the divertor volume. These results confirm the compatibility of H-mode operation with tungsten PFCs, particularly under RMP application and radiative divertor operation, which are both essential for ITER divertor heat load control strategy. The field line penetration depth of splitting lobes proximate to the impurity injection location emerges as a critical factor in optimizing the reduction of steady-state divertor flux. These findings advance the understanding of both the physics underlying divertor control in 3D magnetic geometries and the influence of ITER W main wall on the confinement as proposed in the ITER new baseline.

ACKNOWLEDGEMENTS

This work is supported by the National Key R&D Program of China under Grant No. 2024YFE03270600, the Natural Science Foundation of Anhui Province under Grant No. 2208085J39, the National Natural Science Foundation of China under Grant No. 12005261 and No. 11875292. We thank the staff members at EAST (https://cstr.cn/31130.02.EAST), for providing technical support and assistance in data collection and analysis. The views and opinions expressed herein do not necessarily reflect those of the ITER Organization.

REFERENCES

- [1] A. Loarte et al. "Chapter 4: Power and particle control". In: Nuclear Fusion 47.6 (2007), S203.
- [2] Tetsuo Tanabe. "Power Load on Plasma-Facing Materials". In: *Plasma-Material Interactions in a Controlled Fusion Reactor*. Singapore: Springer Singapore, 2021.
- [3] T. E. Evans et al. "Suppression of Large Edge-Localized Modes in High-Confinement DIII-D Plasmas with a Stochastic Magnetic Boundary". In: *Phys. Rev. Lett.* 92 (23 2004), p. 235003.
- [4] V.A. Soukhanovskii et al. "Divertor heat flux mitigation in high-performance H-mode discharges in the National Spherical Torus Experiment". In: *Nuclear Fusion* 49.9 (2009), p. 095025.
- [5] M. Jia et al. "Control of three dimensional particle flux to divertor using rotating RMP in the EAST tokamak". In: *Nuclear Fusion* 58.4 (2018), p. 046015.
- [6] H. Frerichs et al. "Detachment in Fusion Plasmas with Symmetry Breaking Magnetic Perturbation Fields". In: *Physical Review Letters* 125.15 (2020), p. 155001.
- [7] the TCV Team and the EUROfusion Tokamak Exploitation Team et al. "X-Point Target Radiator Regime in Tokamak Divertor Plasmas". In: *Physical Review Letters* 134.18 (2025), p. 185102.
- [8] M. Bernert et al. "X-Point Radiation, Its Control and an ELM Suppressed Radiating Regime at the ASDEX Upgrade Tokamak". In: *Nuclear Fusion* 61.2 (2020), p. 024001.
- [9] H. Sheng et al. "Simultaneous reduction of tungsten and rotation in the core region induced by RMP". In: *Nuclear Fusion* 65.1 (2024), p. 016009.
- [10] Baoguo Wang et al. "Experimental research on the deeply detached X-point radiator regime on EAST". In: *Nuclear Fusion* 65.8 (2025), p. 086004.
- [11] R.D. Monk et al. "Volume recombination and detachment in JET divertor plasmas". In: *Journal of Nuclear Materials* 266-269 (1999), pp. 37–43.
- [12] J. Dominski et al. "Gyrokinetic prediction of core tungsten peaking in a WEST plasma with nitrogen impurities". In: *Nuclear Fusion* 65.1 (2024), p. 016003.